Authors' Response to Reviews of

A Climate Data Record of Sea Ice Age Using Lagrangian Advection of a Triangular Mesh

Anton Korosov, Léo Edel, Heather Regan, Thomas Lavergne, Emily Jane Down, Signe Aaboe *Earth System Science Data*, ESSD-2025-477

RC: Reviewers' Comment, AR: Authors' Response, \Box Manuscript Text

We are grateful to the reviewers for a comprehensive review of our manuscript and detailed comments!

1. Anonymous referee #1

1.1. Major to moderate comments

RC: (1) Section 3.4 Mapping between the advected meshes

Eq. 5 and 6 suggest a fraction conservation during changes in the areal content (changes proportional to areal change). This can be the case during divergence, but during convergence and hence ice ridging this may not work. This scheme explicitly assumes the ridging intensity to be the same for different age classes. This is in general not the same as younger/thinner ice types have a higher chance for ridging during convergence.

The authors are entirely correct in their statement in Lines 185-186 that there is no straightforward way to account for this based on observations alone. It is not unlikely however that the discrepancies with other products can partly be a result of this equal scaling of fractions of different ages. This is a statement worth making in the text.

AR: Yes, we agree that not accounting for different convergence rates for different ice age fractions can be one of the reasons for the discrepancies. The following text is added in Results and discussions, at the end of a new sub-section **4.2 Comparison of LM-SIAge, NSIDC and SIType datasets**

Several factors lead to the discrepancies observed between the LM-SIAge, NSIDC and SIType products. Firstly, the LM-SIAge and NSIDC are derived from MYI advection, whereas SIType is a radiometric product. Next, LM-SIAge and NSIDC use quite different ice drift products, advection schemes, and representations of the ice age state. In addition, LM-SIAge provides the MYI concentration for each pixel. Summing the areal coverage of MYI, weighted by its concentration, gives the total MYI area. In contrast, NSIDC and SIType products provide a categorical classification, assigning a fixed ice-age class to each pixel. In these cases, the total MYI coverage is obtained by summing the areas of all pixels classified as MYI, which corresponds more closely to an MYI extent. As a result, the ice extent is generally larger than the ice area.

Finally, we don't account for different convergence (and melting) rates of ice of different ages, as we cannot constrain that by observations (see Eq. 5). Assuming that older ice is thicker and can converge (melt) less than the thinner younger fractions, we may overestimate the loss of older ice in converging (melting) cells. Our previous experiments with a numerical model-based estimate of sea ice age (Reagan et al., 2023) indicate that ridging younger ice first yields more realistic estimates of MYI extent. However, that may lead to an underestimation of MYI ridging in areas where MYI and

FYI thicknesses are similar (e.g., the marginal ice zone) and in recent years, as MYI thins out faster than FYI (Kwok et al., 20018).

RC: (2) Uncertainty calculations.

Section 3.8 begins with presentation of "The uncertainty of the produced sea ice age variable". Please clarify what is "sea ice age variable". Is it something related with Eq.(11)? If this is the case, then (if I don't misunderstand something), Eq.12 does not seem to be correct - it is not just a sum of uncertainties scaled by the respective ages. Uncertainty of the weighted average can be calculated by the error propagation formula (can be found elsewhere).

AR: Yes, indeed, we did not account for division by the sum of concentrations. The error propagation formula in the case of division/multiplication reads as follows:

$$\left(\frac{\sigma_q}{q}\right)^2 = \left(\frac{\sigma_x}{x}\right)^2 + \left(\frac{\sigma_y}{y}\right)^2,\tag{1}$$

where q=x/y. I.e., $x=\sum_{i=0}^N A_i C_{iY}, y=\sum_{i=0}^N C_{iY}, \sigma_x^2=\sum_{i=0}^N A_i * \sigma_{C_{iY}}^2, \sigma_y^2=\sum_{i=0}^N \sigma_{C_{iY}}^2$. The equation is corrected in the text, and the uncertainties are recalculated in the product.

RC: Need to mention that this section is quite difficult to read/comprehend. Can the authors consider adding another figure similar to Figure 2 where the entire sequence of uncertainty calculation/aggregation is presented? As far as I see the authors assume the uncertainties for concentrations/fractions for different age classes to be independent?

AR: The uncertainty computation section is rewritten from deductive (from general principles to specific conclusions) into inductive (from specific details to general conclusions) logic for easier understanding. A flowchart with an uncertainty estimation algorithm is added (see Fig. 1 below). Yes, we assume the uncertainties are independent because we don't have a method to compute their covariations. This is indicated at the beginning of the section.

RC: The uncertainties, the way they are presented in the data (%) and in e.g. Figure 8, are these absolute values (i.e. ice concentrations) or % of these fractions/concentrations? What is the "total uncertainty" – sum of uncertainties for all ice fractions? Please clarify.

AR: These are absolute values, concentrations. The following clarification is added to the figure caption:

SIC uncertainties are provided as absolute values of concentration.

RC: The authors apply caping to advected concentrations. Did the authors consider applying the same procedure (caping/or better say conditioning) to the uncertainties? The total uncertainty looks higher than the observed SIC uncertainty.

AR: In case of conditioning, we keep the minimal value of the two concentrations. We therefore have to take the full uncertainty of the value we keep, not the minimum of the two uncertainties. The total uncertainty (i.e., left column in Figs. 8 and 9) is a combination of SIC uncertainty (the second column) and SID uncertainty (fourth column), and is therefore larger than both of them (See Eq. 15). As the uncertainty computation section is completely rewritten, it is easier to understand the relation between the uncertainties presented in Figs. 8 and 9.

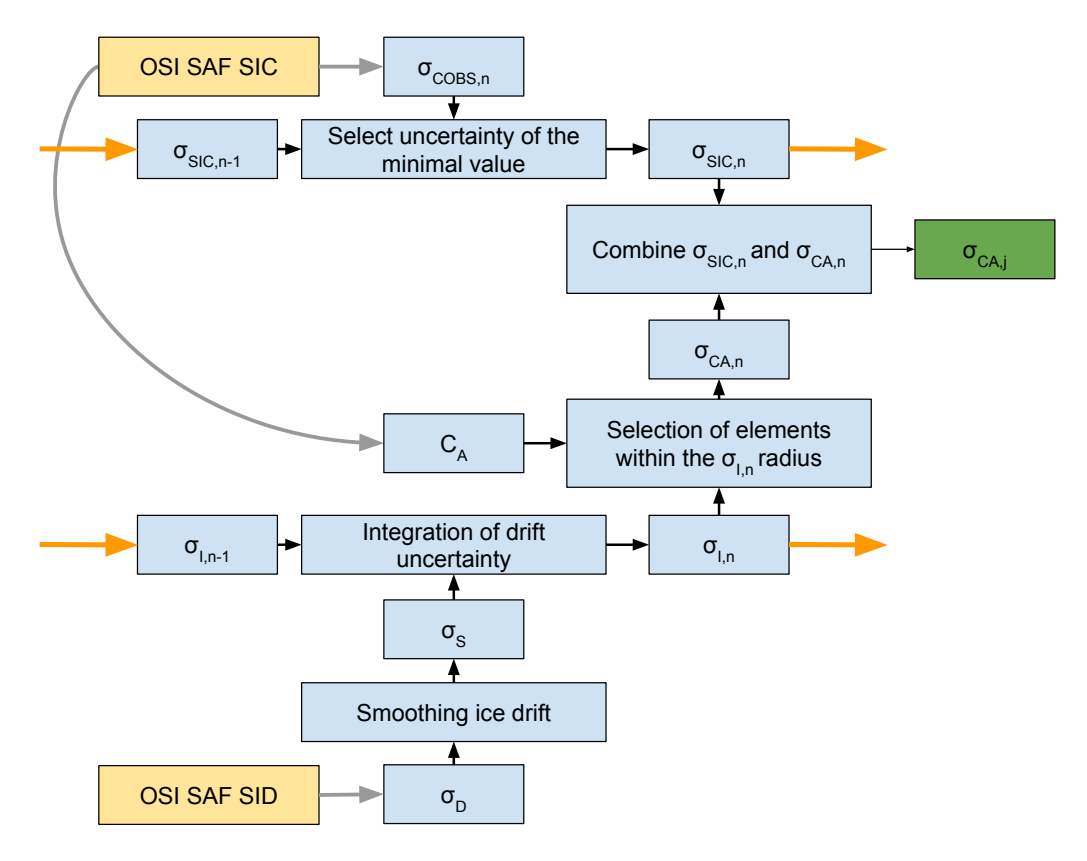


Figure 1: Flowchart of computing uncertainty of an advected MYI fraction $\sigma_{CA,j}$ (Eq. 15). Input data is shown in yellow, the final result is shown in green. The orange arrows indicate data flow using the advected mesh. See Eqs. 11 - 19 for notation of individual uncertainty components.

1.2. Minor comments

- RC: (1) According to WMO nomenclature, see 2.6.1 in https://cryo.met.no/sites/cryo/files/ IceService_docs/WMO_259-2015_multilingual.pdf FYI ice that survived the summer minimum is called "residual ice" and it "officially" turns into SYI only on the 1 January of the coming winter. I understand that it makes it much easier for understanding if the indexing is changed in the way the authors did, but good to mention, at least, that you bypass the established classification a bit.
- AR: The following text is added in Section 3.1, after Eq. 2:

It should be noted that according to the nomenclature of the World Meteorological Organisation (Sea Ice Nomenclature, WMO-259), the first-year ice (FYI) that survives the summer minimum is called "residual ice" and it turns into second-year only on 1 January of the coming winter. Nevertheless, hereafter, all survived FYI turns into second-year after 15 September.

- RC: (2) Figure 2: please add colorbars to the panels to improve the visualization. Consider also adding notation like "step 1", "step 2" (or just subplot numbers) in the figure and in the corresponding text in Lines 113->
- AR: Two colobars (for the advected and computed concentrations) are added to the figure. Notation of steps is added to the figure and is referenced in the accompanying text.
- **RC:** (3) Figure 15: please clarify what the numbers on the colorbars denote.
- AR: The following clarification is added to the figure caption:

SIC uncertainties are provided as absolute values of concentration.

2. Anonymous referee #2

- RC: (1) One thing that I was concerned about was a validation and uncertainty analysis of the constructed dataset. The authors used buoy position data to validate the age product. It is an acceptable approach. However, the used buoy trajectories cover only between 2002 and 2024. The product for the earlier period of 1991 2011 was not validated in this manuscript. The uncertainty inherent in this product depends on the quality of the passive microwave-based SICs. The uncertainty of SICs can vary with seasons. The seasonal uncertainties of the age product due to the SIC uncertainties should be addressed. In addition, the uncertainty section is difficult to read and understand. I recommend reformulating this section.
- AR: The buoy database is extended to start from 1991, and the validation results are updated. The uncertainty computation section is rewritten from deductive (from general principles to specific conclusions) into inductive (from specific details to general conclusions) logic for easier understanding. A flowchart with an uncertainty estimation algorithm is added (see Fig. 1). Analysis of seasonal variations of uncertainty is added as a sub-section in Results:

4.3 Seasonal and interannual variations of uncertainty

We analysed the variability of average uncertainty in the source data and in the derived dataset (see Fig. 2). The observed SIC uncertainty ($\sigma_{C_{OBS}}$, Fig. 2, A) shows strong seasonal variations, with a minimum ($\approx 2\%$) in winter and a maximum ($\approx 4.5\%$) during the melt season. The observed SID uncertainty (σ_S , Fig. 2, B) also has a minimum (≈ 3.5 km d⁻¹) in winter, a plateau of constant values

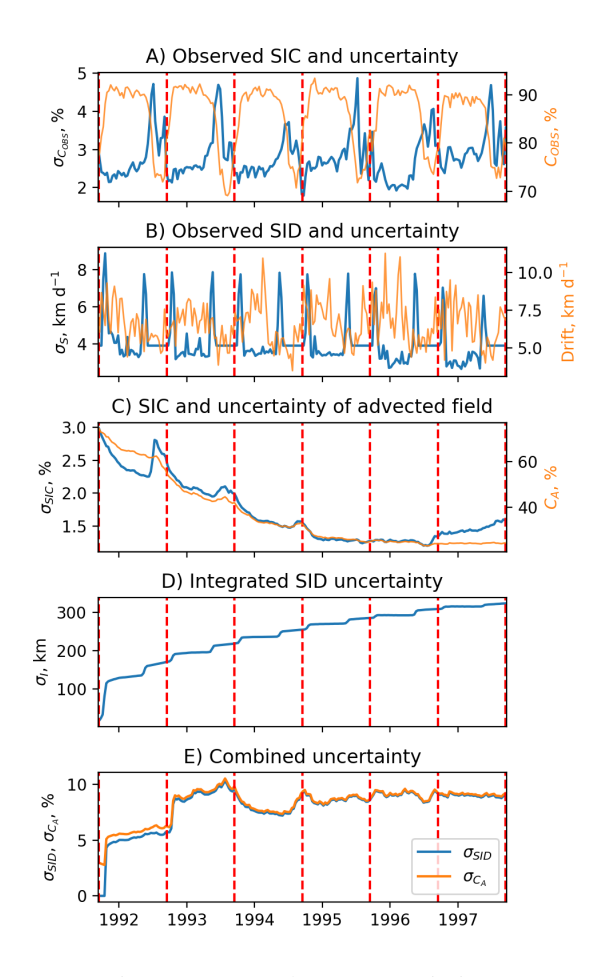


Figure 2: SIC and SID uncertainties.

of 4 km d⁻¹ in summer, and two peaks with \approx 7 km d⁻¹ just before and after the summer period. The uncertainty of the advected MYI field (σ_{SIC} , Fig. 2, C) starts from \approx 3% and gradually decreases over 6 years, with a slight increase during summer seasons. The integrated uncertainty of ice drift (σ_I , Fig. 2, D) starts from nearly zero and increases step-wise following the pre- and post-summer peaks of σ_S . The uncertainty of advected MYI concentration, associated with the uncertainty of ice drift (σ_{SID} , Fig. 2, E), also begins low and then rapidly increases during the first year, which is followed by a gradual increase during consecutive years with strong seasonal variations. The total uncertainty of the advected MYI field (σ_{CA} , Fig. 2, E) is first dominated by the uncertainty in the observed SIC, but after the end of the melt season and the jump of σ_S , the contribution of σ_{SIC} becomes much less pronounced.

RC: (2) In methodology, the authors chose certain parameters, e.g., mesh element size thresholds, angle, and element area, which seem to be used without any justification. It would be better if the authors provide how sensitive the results are changed due to these parameters or references to support these values.

AR: Values for these parameters are chosen to keep the size of the mesh elements similar to the resolution of the destination grid (i.e., $\Delta x = \Delta y = 25$ km). Smaller parameter values yield smaller elements and do not change the results, but they require much more CPU time for advection and, especially, remeshing. Larger values/elements lead to a lower effective resolution of the product (neighbour pixels on the destination grid have the same values. The following clarification is added after the parameter values are listed:

The end results are not very sensitive to the mesh size, and these parameter values are chosen to keep the area of the mesh elements below the area of the destination grid elements with a spatial resolution of 25 km, and to keep the elements large enough for efficient advection and, especially, time-consuming remeshing.

- RC: (3) Are there any possibilities of ridging or deformation processes with different age categories affecting the proposed algorithm?
- AR: Yes, not accounting for different convergence rates for different ice age fractions can be one of the reasons for the discrepancies. The following text is added in Results and discussions, at the end of a new Sub-section **4.2** Comparison of LM-SIAge, NSIDC and SIType datasets

Several factors lead to the discrepancies observed between the LM-SIAge, NSIDC and SIType products. Firstly, the LM-SIAge and NSIDC are derived from MYI advection, whereas SIType is a radiometric product. Next, LM-SIAge and NSIDC use quite different ice drift products, advection schemes, and representations of the ice age state. In addition, LM-SIAge provides the MYI concentration for each pixel. Summing the areal coverage of MYI, weighted by its concentration, gives the total MYI area. In contrast, NSIDC and SIType products provide a categorical classification, assigning a fixed ice-age class to each pixel. In these cases, the total MYI coverage is obtained by summing the areas of all pixels classified as MYI, which corresponds more closely to an MYI extent. As a result, the ice extent is generally larger than the ice area.

Finally, we don't account for different convergence (and melting) rates of ice of different ages, as we cannot constrain that by observations (see Eq. 5). Assuming that older ice is thicker and can converge (melt) less than the thinner younger fractions, we may overestimate the loss of older ice in converging (melting) cells. Our previous experiments with a numerical model-based estimate of sea ice age (Reagan et al., 2023) indicate that ridging younger ice first yields more realistic estimates of MYI extent. However, that may lead to an underestimation of MYI ridging in areas where MYI and FYI thicknesses are similar (e.g., the marginal ice zone) and in recent years, as MYI thins out faster than FYI (Kwok et al., 20018).

- RC: (4) It is very fair to provide Figure 15 for the NSIDC product as well.
- AR: The NSIDC age product is validated against the IABP data using the same methodology as for the LM-SIAge product (see Fig. 3 below). There are fewer correct predictions of the maximum ice age in the NSIDC product than in the LM-SIAge. Moreover, collocations of IABP buoys younger than 1 year with corresponding NSIDC estimates are almost absent, suggesting a positive bias in the NSIDC product. The following text is added in the abstract:

Validation with IABP buoys indicates good consistency (LM-SIAge does not underestimate max age of the buoys in 96.6%), with most discrepancies occurring near the ice edge. The NSIDC product does not underestimate the age only in 94% and potentially underestimates the presence of FYI.

The following text is changed in the section **3.9 Validation**:

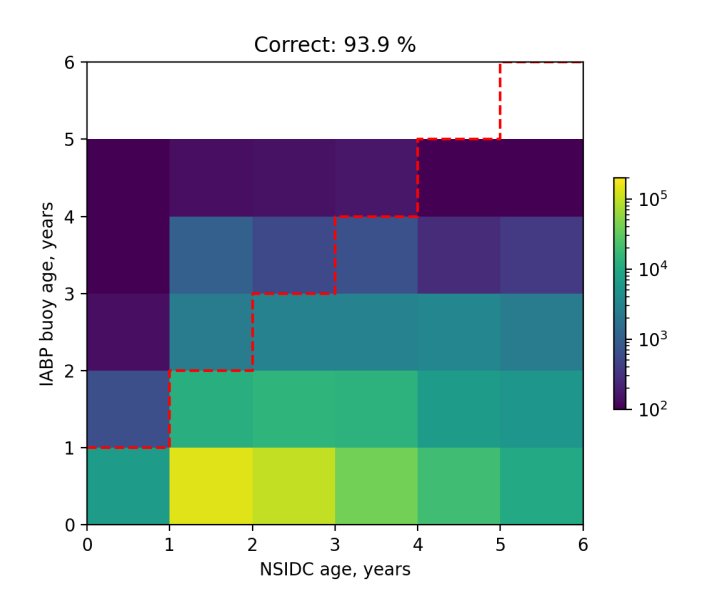


Figure 3: Validation of the NSIDC ice age product on IABP data.

For validation of the LM-SIAge product and NSIDC products, we used trajectories of sea ice drifting buoys from the IABP dataset. We compare the maximum ice age detected by LM-SIAge the Lagrangian algorithms to the age of the ice drifting buoys.

The following text is added in the section **4.3 Validation results**:

The NSIDC product does not underestimate the buoy age only in 94% (see Fig. 15, D). Comparing 2D histograms on Fig. 15 B and D, we observe a significantly lower number of match-ups in the NSIDC FYI category, confirming that this product tracks the maximum age in a grid cell and potentially underestimates the presence of FYI.

RC: (5) In supplementary videos, I found that somewhat permanent multiyear ice exists in the coastline of the Kara Sea and Islands between the Kara and Laptev Seas. Is this correct?

AR: Thank you for spotting this! MYI is not expected to appear that far south. However, this is not an error in the Lagrangian advection algorithm. That happens because non-zero sea ice concentrations are present in the upstream SIC CDR product year-round due to, most likely, the spill-over effect. We added a flag to the output product indicating which pixels are likely affected by this effect and may have falsely high MYI concentrations. The following text was added to sub-section **4.2 Comparison of LM-SIAge, NSIDC and SIType datasets**:

One minor difference between the LM-SIAge and NSDIDC products, which is hard to spot, is the presence of MYI near the coast in the Kara and Laptev seas (also seen on the supplementary videos). This is not realistic and results from enhanced sea ice concentrations near the coast in the upstream

SIC products due to the "land spillover" effect (Kern et al., 2022). These pixels are masked in the netCDF files.

3. Anonymous referee #3

3.1. Specific comments

RC: Section 3.1 – Representation of Age Evolution

The computation of sea-ice age change appears to assume that all ice categories evolve similarly in time. In reality, when sea-ice concentration decreases, younger ice tends to melt more rapidly than older ice. It would be helpful if the authors could clarify whether this differential melting behavior is accounted for in their formulation, or discuss its potential implications for the resulting age distribution.

AR: Indeed, not accounting for different convergence and melting rates for different ice age fractions can add a bias to the age distributions. The following text is added in Results and discussions, at the end of a new Sub-section 4.2 Comparison of LM-SIAge, NSIDC and SIType datasets

Several factors lead to the discrepancies observed between the LM-SIAge, NSIDC and SIType products. Firstly, the LM-SIAge and NSIDC are derived from MYI advection, whereas SIType is a radiometric product. Next, LM-SIAge and NSIDC use quite different ice drift products, advection schemes, and representations of the ice age state. In addition, LM-SIAge provides the MYI concentration for each pixel. Summing the areal coverage of MYI, weighted by its concentration, gives the total MYI area. In contrast, NSIDC and SIType products provide a categorical classification, assigning a fixed ice-age class to each pixel. In these cases, the total MYI coverage is obtained by summing the areas of all pixels classified as MYI, which corresponds more closely to an MYI extent. As a result, the ice extent is generally larger than the ice area.

Finally, we don't account for different convergence (and melting) rates of ice of different ages, as we cannot constrain that by observations (see Eq. 5). Assuming that older ice is thicker and can converge (melt) less than the thinner younger fractions, we may overestimate the loss of older ice in converging (melting) cells. Our previous experiments with a numerical model-based estimate of sea ice age (Reagan et al., 2023) indicate that ridging younger ice first yields more realistic estimates of MYI extent. However, that may lead to an underestimation of MYI ridging in areas where MYI and FYI thicknesses are similar (e.g., the marginal ice zone) and in recent years, as MYI thins out faster than FYI (Kwok et al., 20018).

- RC: Clarity of Method Description (Figures 5 and 6)
 - Since the triangular-mesh approach and its associated remeshing procedure may be unfamiliar to many readers, the description of these processes could be improved for clarity. Figures 5 and 6 are central to understanding the proposed algorithm, but both could be made more legible and intuitive.
- AR: Figure 5 and 6 were updated according to the specific comments below (see Figs. 4 and 5). References to specific panels on figures 5 and 6 were added to the text for clarity.
- RC: In Figure 5, particularly in the left and right examples, it is difficult to visually identify what has changed before and after the remeshing process. The green lines representing the remeshed state are also hard to distinguish.
- AR: Descriptive labels were added to Figure 5 for easier understanding, and the green colour was changed to

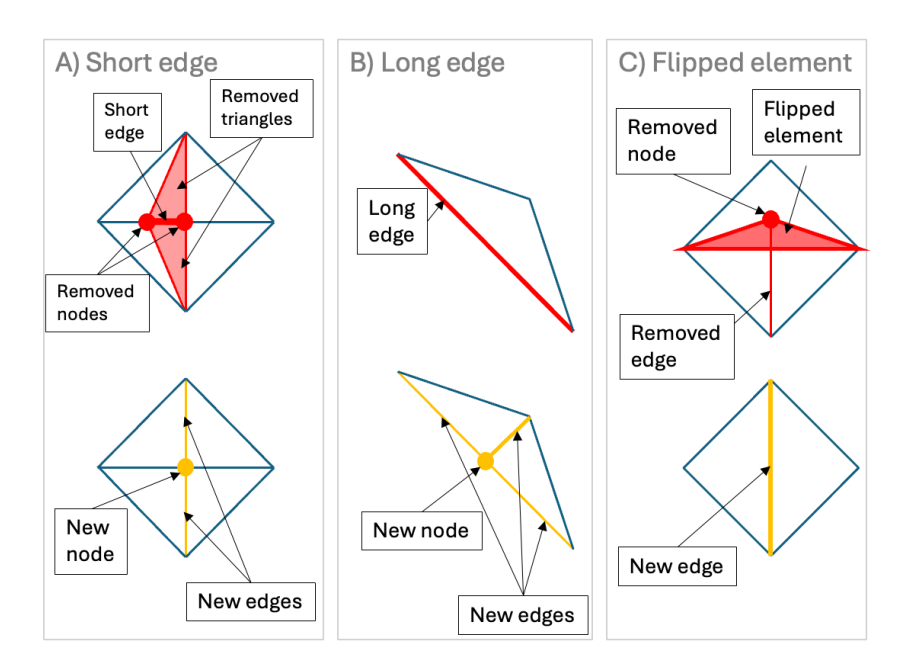


Figure 4: Scheme of three types of remeshing: collapsing of a short edge (A), splitting of a long edge (B), removing a flipped element (C). Edges and elements before remeshing are shown in red in the upper row, and the new mesh is shown in yellow in the lower row.

yellow (see Fig. 4 below).

RC: In Figure 6, the blue and black lines in the left panel are not easily distinguishable. Enhancing the color contrast or line thickness would improve readability.

AR: Three panels in Figure 6 were replaced with four panels, illustrating the advection/remeshing/optimisation processes in more detail and using only two colours for clarity (see Fig. 5 below).

RC: Adding brief explanatory captions to Figures 5 and 6 that summarize what each step represents (e.g., "before remeshing," "after remeshing," "regularized mesh") would help non-specialist readers.

AR: Clear indication of remeshing process steps is added to the figures and their captions (see Figs. 4 and 5 below).

4. Handling topic editor, Clare Eayrs

4.1. Uncertainty quantification and presentation

RC: All reviewers found the section on uncertainty difficult to follow. Please reformulate this section and consider adding a flowchart or schematic that illustrates the complete sequence of uncertainty estimation. Please define exactly what is meant by "sea ice age variable" and explain how uncertainties are calculated and combined.

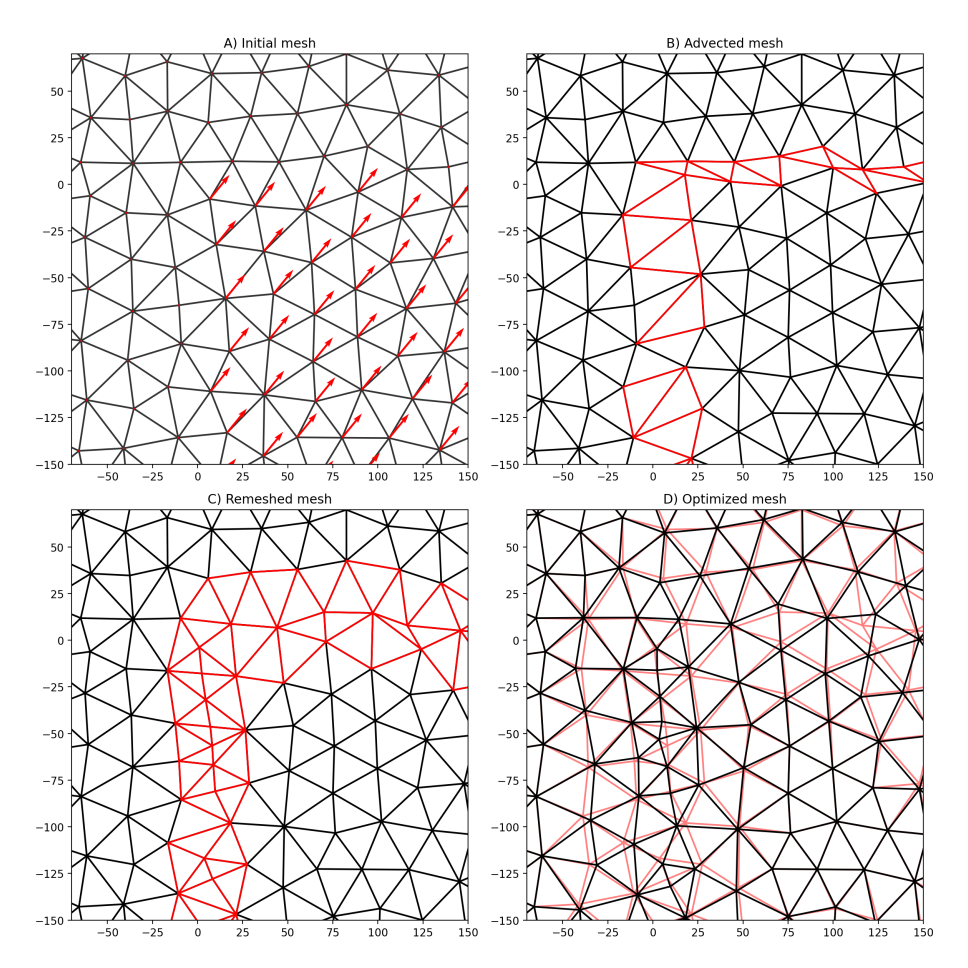


Figure 5: Illustration of the node advection and mesh optimisation process. A) Some nodes of the initial mesh (shown in black) are advected using ice drift vectors (shown in red). B) The advected mesh (shown in black) has some distorted elements that require remeshing (shown in red). C) Most of the elements on the remeshed mesh remain unchanged (shown in black). The new elements introduced by remeshing are shown in red. D) Position of the nodes in the remeshed mesh is updated, and a regularised mesh is created (shown in black). The previous mesh (remeshed, but not regularised, shown in red) differs from the optimised one only near the new elements, in the vicinity of the convergence/divergence zone. In contrast, in the homogeneous ice-drift area (lower right corner), the advected mesh is equal to the remeshed and optimised meshes.

- AR: The uncertainty computation section is rewritten from deductive (from general principles to specific conclusions) into inductive (from specific details to general conclusions) logic for easier understanding. A flowchart with an uncertainty estimation algorithm is added (see Fig. 1). Only a flowchart is provided in the current response, and the rewritten section will be submitted with the revised manuscript.
- RC: If the uncertainty varies spatially and temporally, please provide the uncertainty as a separate data file that matches the spatial and temporal dimensions of your primary product, and document how users should apply the uncertainty information.
- AR: The spatially and temporally varying uncertainty is already provided together with the product. For convenience, it is included in the data files, as specified in Table 1 of the submitted manuscript. In addition, we suggest adding a subsection to Results and discussion that highlights seasonal and interannual variations in uncertainty (see Fig. 2 and our response to refree #3 above).
- RC: Please clarify whether the uncertainties shown in figures are absolute or relative values, and whether the "total uncertainty" represents the sum or the propagated metric. Please also address Reviewer 1's query regarding capping/conditioning of the uncertainty.
- AR: The uncertainties are absolute, and a corresponding notation is added to the figure caption. We addressed the Reviewer 1's query regarding capping and improved explanations in the rewritten section on uncertainty computations.

4.2. Physical assumptions in the algorithm

- RC: Reviewers 1 and 2 both highlighted that your scheme assumes equal scaling of fractions of different age classes. Please discuss the limitations of the mapping approach during convergence/ridging and how the assumption of equal scaling fractions of different age classes could influence the product and comparisons with other datasets. Reviewer 3 also asked whether your formulation accounts for the fact that younger ice tends to melt more rapidly when the concentration decreases. Please clarify whether this differential melting is represented, and if not, what the likely effect is on the age distribution.
- AR: The clarification on how equal convergence and melting of ice of different ages affect the final results has been added.

4.3. Justification for parameter choices

- RC: Please include a justification for the numerical parameters in the mesh set-up and either add references or a brief discussion on the sensitivity of these parameters to support these values.
- AR: The parameter values are chosen using simple geometric and algorithm efficiency considerations. Their values do not significantly affect the results, but may increase processing time or reduce the effective spatial resolution. Corresponding clarifications are added to the text.

4.4. Figures

- RC: Please add labels to colorbars and address the specific review comments.
- AR: The labels and colobars are added as requested. Not all the updated figures are presented in the current response.
- RC: Please specify the DOIs for the OSISAF datasets that the user should download in the README file in

the Zenodo repository. I noticed you recommend the Sea Ice Concentration Climate Data Record Release 3 (OSI-450-a), but this has been superseded by version 3.1 (OSI-450-a1). I strongly encourage the authors to update the sea ice age product to base it on the latest sea ice concentration CDR, thereby making it more useful for downstream users. An update now would also help prevent confusion with future work based on newer data and likely increase the dataset's usage and citations. If this update is not feasible at this stage, it would be helpful to outline any plans for future updates.

AR: The DOIs of the upstream data products are added to the Zenodo README. The current dataset was produced before SIC CDR v3.1 was available. Unfortunately, it is not feasible to switch to a new version because downloading and reprocessing would require resources we do not currently have. We are running a project that provides funding to improve algorithms and extend the dataset to include data through 1978. Understandingly, this process will take some time. We, therefore, would like to publish the dataset as is, with a minor update to flag spurious MYI. The following text is added in Conclusions regarding our plans for future updates:

In future, it is planned to improve the Lagrangian advection algorithm, include newer upstream CDRs, back-extend the time series up to 1979, and cover the Southern Ocean.